ACS Synthetic Biology

pubs.acs.org/synthbio
Research Article

Evaluating Apoptotic Gene Efficiency for CHO Culture Performance Using Targeted Integration

David Catalán-Tatjer, Saravana Kumar Ganesan, Iván Martínez-Monje, Lise M. Grav, Jesús Lavado-García,* and Lars K. Nielsen

Cite This: ACS Synth. Biol. 2025, 14, 1414−1424
Read Online

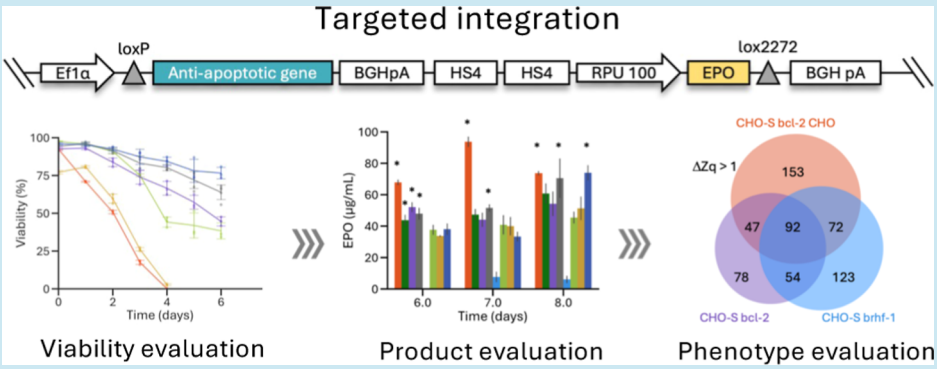

ABSTRACT: Chinese hamster ovary (CHO) cells have long been the favored platform for producing complex biopharmaceuticals, such as monoclonal antibodies. Cell death is a critical factor in all CHO cultures, dictating the duration until harvest in batch cultures and viable cell density in perfusion. The programmed cell death, or apoptosis, pathway has been widely studied due to its relevance in affecting cell culture performance and the extensive knowledge about its protein-to-protein interaction network. However, clonal variation seen with random integration has confounded results, and it remains unclear which effector genes should be overexpressed. Here, we employed the recombinase-mediated cassette exchange strategy to develop isogenic cell lines expressing one copy of erythropoietin, as a model protein product, and various antiapoptotic genes: bcl-2 from CHO and human origin, bcl-xL from CHO and human origin, mcl-1, and bhrf-1. We tested the generated isogenic cell lines in the presence of sodium butyrate, a well-known apoptotic initiator, in a batch culture. The most promising candidates were cultured in fed-batch in the microbioreactor ambr15 system. The observed phenotype varied significantly depending on the overexpressed gene; therefore, the metabolic differences were further characterized using multiplexed quantitative proteomics. We showed that overexpressing bcl-2 from the CHO origin significantly improved productivity and established a methodology to successfully test candidate genes via targeted integration. This will enable future metabolic engineering strategies to be more comparable and overcome the challenges faced thus far.

KEYWORDS: *targeted integration, CHO cells, antiapoptosis*

INTRODUCTION

Programmed cell death or apoptosis represents the culmination of a signaling cascade activated during periods of heightened cellular stress, stemming from factors such as mechanical or oxidative stress, as well as nutrient depletion.[1−3] The loss of cell viability ultimately dictates when batch cultures are terminated; hence, many studies have been dedicated to studying and delaying apoptosis as much as possible, following the guiding principle of "the longer the culture, the higher the productivity".[4,5] The first exponent of this idea was the introduction of the fed-batch culture, in which limiting nutrients were supplemented while the culture was already growing and producing, aiming to delay the apoptosis triggered by the absence of these key nutrients.[6,7] Alongside the fed-batch, perfusion mode has been used to extend cultures for prolonged periods of time[8] while achieving record-high cell density, constrained by nutrient and oxygen supply to the culture.[8−10] Even perfusion, however, is affected by apoptosis as the bleeding rate is directly linked to the death rate, varying in the achieved pseudo steady-state.

Apart from feeding strategies to mitigate nutrient depletion,[11] numerous scientists have explored various genetic engineering approaches to delay apoptosis. Recently, hybridoma and

Received: May 31, 2024
Revised: March 21, 2025
Accepted: March 26, 2025
Published: April 23, 2025

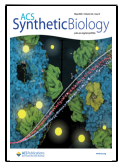

https://doi.org/10.1021/acssynbio.4c00382
ACS Synth. Biol. 2025, 14, 1414−1424

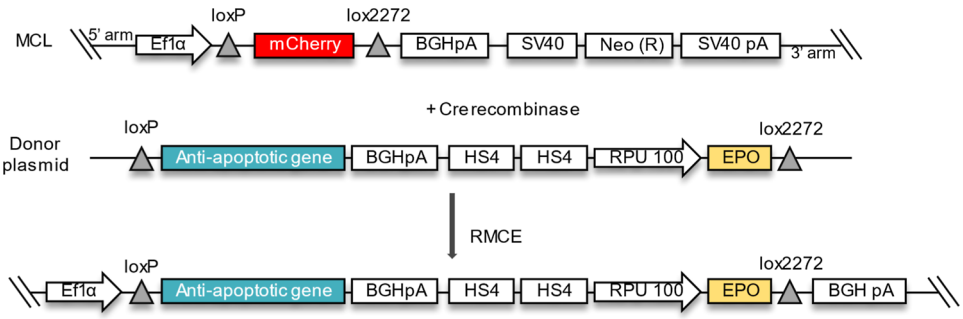

Figure 1. Isogenic cell line generation strategy. CHO−S MCL was transfected with two plasmids: a Cre recombinase plasmid and a donor plasmid. The donor plasmid was designed with the corresponding antiapoptotic gene followed by the bovine growth hormone polyadenylation signal (BGHpA) and by two copies of chicken β-globin locus control region hypersensitive site 4, which act as an insulator to enhance EPO expression. RPU 100 was selected as a promoter for EPO. LoxP sequence was added on the 5′ arm of the construct, whereas lox2272 was located at 3′ arm. After dual transfection, cells were sorted based on mCherry fluorescence.

Chinese hamster ovary (CHO) cells were engineered to overexpress or knock out (KO) apoptotic-related genes.[3,12,13] Henry et al. reviewed the impact of bcl-2 family proteins, which includes Bax, Bak, bcl-2, bcl-xL, and mcl-1, on CHO cells as they have been the most studied regarding apoptosis delay.[14] Bax and Bak function as effector proteins capable of inducing pores on the mitochondrial membrane, thereby initiating apoptosis. Conversely, bcl-2, bcl-xL, and mcl-1 serve as inhibitor proteins, impeding the generation of these pores.[14] Many publications report that overexpressing either bcl-2, bcl-xL, mcl-1, or a combination of them led to higher final titers as apoptosis was significantly delayed.[15,16] Other studies report on KO Bax and/or Bak to prevent apoptosis with promising results.[12,17] Furthermore, considering the impact of these proteins on the mitochondrial membrane and, consequently, their influence on the efficiency of the electron transport chain and the tricarboxylic acid (TCA) cycle, some researchers have evaluated these cell lines with regard to these specific pathways with interesting results.[18] Similar studies were performed in murine hybridoma cells in which both bhrf-1, an Epstein−Barr virus-encoded early protein with structural and functional homology with the antiapoptotic protein bcl-2, and bcl-2 were overexpressed and compared, improving cell survival and, consequently, productivity in both batch and continuous processes.[19]

Regarding the success of these strategies and the development of advanced techniques for cell line generation, scientists have tried to replicate and improve previously reported data, with contradicting results as compiled by Henry et al.[14]

For instance, while some authors describe an increase in the specific productivity (q_p) when overexpressing bcl-xL,[20] other studies conclude that there was no significant change.[21] Similar discrepancies have been reported with bcl-2. Additionally, not all publications regarding the improvement in the duration of the culture agreed on the beneficial effects on the expression of either bcl-2 or bcl-xL.

This lack of reproducibility and discrepancy in the reported works might be attributed to clonal variation. The use of random integration to generate stable cell lines[16,22,23] is associated with large clonal variation, and it is uncommon to characterize tens of strains to accommodate for this variation. Conversely, the study of cell pools suffers from a diffuse signal, particularly if exposed to an extended batch culture. This concern was already highlighted by Henry et al., who concluded that establishing isogenic cell lines in a stable genomic location may be the only viable option to ensure meaningful comparisons.[14]

As implied by Henry et al.,[14] we used, for the first time, an isogenic cell line strategy[24] to evaluate the antiapoptotic genes bcl-2 and bcl-xL from human origin, bcl-2 and bcl-xL from CHO origin, mcl-1, and the apoptosis regulator bhrf-1 from Epstein−Barr virus. Targeted integration was used to develop isogenic cell lines expressing one copy of each relevant gene to overcome clonal variation. In order to test the hypothesis related to productivity, one copy of erythropoietin (EPO) was integrated by using the same strategy. This work, to the best of our knowledge, is the first to use isogenic cell lines to compare the expression of several antiapoptotic genes. With this experimental design, we aim to provide a reliable study regarding antiapoptotic genes and their effect on culture performance to the scientific community.

RESULTS AND DISCUSSION

Successful Generation of Stable Isogenic Subclones Coexpressing EPO and Antiapoptotic Genes. Clones generated via recombinase-mediated cassette exchange (RMCE) share the same genome and, therefore, can be termed isogenic. Consequently, we do not anticipate any significant differences between isogenic clones when assessing cell growth, metabolism, and production.[25] This enables meaningful comparisons regarding the effects of gene expression as it ensures that each gene is present in one copy under the same promoter and in the same gene location across all cell lines. However, epigenetic changes and varying stress conditions can lead to subtle differences between subclones.

A CHO master cell line (MCL) with an already integrated single landing pad previously generated by our group[24] was used to create the different isogenic cell lines harboring antiapoptotic genes (Figure 1).

We successfully generated and verified a minimum of three subclones for each cell line coexpressing one copy of the antiapoptotic gene and one copy of EPO. All donor plasmids employed in this step are described in Figure S1.

The process of clone validation began with junction PCR to verify the expected size of the inserted construct. Recognizing the potential for recombination to occur at other genomic sites, a subsequent step was required to detect any additional recombination events. Therefore, quantitative PCR (qPCR) was utilized to assess the number of EPO copies present in the entire genome. Clones that underwent positive junction PCR validation and possessed a single copy of EPO (Figure S2) were banked and characterized. A negative control was generated with

https://doi.org/10.1021/acssynbio.4c00382
ACS Synth. Biol. 2025, 14, 1414−1424

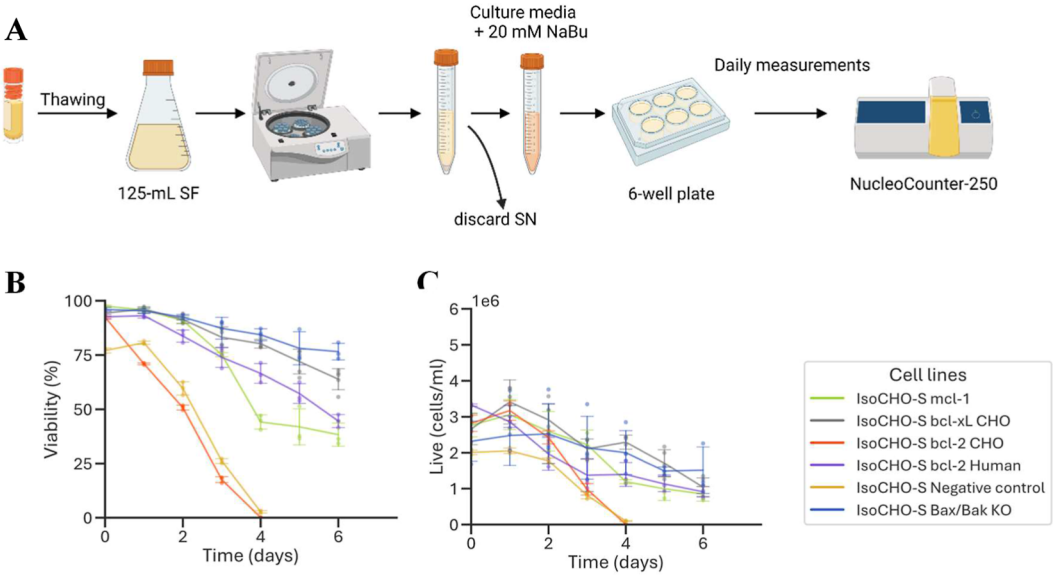

Figure 2. (A) Cells were carefully thawed transferring the content from a cryovial containing 10×10^6 cells to a 125 mL shake flask with a working volume of 30 mL. Then, cells were resuspended in culture media supplemented with 20 mM of NaBu to reach a final concentration of 2.5×10^6 cells/mL in 3 mL of working volume in a 6-well plate. (B) Viability assessment and (C) cell counts were performed with the NucleoCounter.

the same methods, replacing the antiapoptotic gene with 3 STOP codons in the donor plasmids (Figure S1).

A positive control was generated by KO the bcl-2 family effector proteins Bax and Bak, which are pivotal in pore formation in the mitochondrial membrane, triggering apoptosis. The KOs were performed in the negative control cell line and successfully confirmed by Western blot (Figure S3).

Antiapoptotic Isogenic Cell Lines Were Able to Withstand the Toxic Effect of Sodium Butyrate. We studied the performance of the developed cell lines with sodium butyrate (NaBu) as it is commonly used in cell cultures to boost productivity but will induce apoptosis at elevated concentrations.[26,27] Therefore, a cell line able to better withstand the negative impact of NaBu while keeping cells viable for a longer time will be industrially relevant. For that reason, we examined the culture progression of three isogenic clones each for isoCHO-S mcl-1, bcl-xL CHO, bcl-2 CHO, bcl-2, and positive control BaxBak KO compared to the negative control upon incubation with 20 mM NaBu (Figure 2A). All bcl-2 genes except bcl-2 CHO significantly delayed cell death compared to the negative control (Figure 2B) with comparable performances in the viable cell density (VCD) progression (Figure 2C). As expected, the positive control BaxBak KO showed the greatest degree of protection.

The inability of bcl-2 CHO to suppress apoptosis was unexpected (Figure 2B). We first compared the cloned sequence with the native genes in Chinese hamsters and humans to rule out a deleterious mutation in the isoCHO-S gene. The cloned gene was identical to the Chinese hamster gene (Uniprot ID Q9JJV8), which is homologous to the human bcl-2 alpha isoform (P10415-1), except for a three-amino-acid insertion in the latter. Of 25 single amino acid differences between Chinese hamster and human, 17 are identical with those of the mouse instead (P10417). In proteomics (see later), bcl-2 CHO and human bcl-2 were quantified using identical peptides, and their expression was comparable. We conclude that the relatively small changes in the sequence could be responsible for the different profiles observed.

This significant effect caused by a small genetic difference may explain the inconsistent results in previous studies. Five out of 13 previous experiments reviewed by Henry et al. observed no effect when bcl-2 was overexpressed, while the remaining eight experiments reported an improvement of at least 1 day.[14] This highlights the value of using isogenic cell lines when genes are capable of displaying subtle effects.

This study showed promising results for all antiapoptotic cell lines, except for bcl-2 CHO. In addition to the small genetic differences between CHO and human bcl-2, this behavior may be a consequence of the impact of NaBu on cell metabolism, as the molecular mechanisms underlying these improvements remain poorly understood.[28] Nevertheless, the results shown in Figure 2A,B highlight the potential and the need to further explore the isoCHO-S cell lines generated in this work.

Isogenic CHO−S Bcl-2 CHO Achieved the Highest Titer, whereas isoCHO-S Bcl-2 Showed the Longest Batch Culture Time. While convenient, NaBu stress is artificial and does not capture the cellular stress observed in most cultures. We next compared the effect of overexpressing bcl-2 genes in conventional batch cultures over a span of 9 days with three subclones for each cell line. Two additional genes were included in the comparison: bhrf-1 is the bcl-2 homologue originating from the Epstein−Barr virus, while bcl-xL is the human version of bcl-xL allowing another comparison between human and CHO bcl-2 family genes.

Apart from isoCHO-S bhrf-1, all cell lines, including positive and negative controls, displayed similar development in batch until day 6 (Figure 3). While isoCHO-S bhrf-1 and isoCHO-S mcl-1 achieved the maximum cell density (Figure 3A), this was countered by small differences in cell diameter (Figure 3C), and the metabolic profiles were nearly identical, with depletion of glutamine at day 4 (Figure 3D) and glucose at day 5 (Figure 3E). From day 6 to day 7, VCD and viability of isoCHO-S bcl-2 CHO experienced a precipitous decline, reducing viability by 50%, distinguishing it as the poorest-performing cell line (Figure 3B), mirroring its performance upon NaBu addition. Conversely, human bcl-2 showed the slowest decline. isoCHO-S bhrf-1 and isoCHO-S mcl-1 achieved the highest cell density (Figure 3A)

https://doi.org/10.1021/acssynbio.4c00382
ACS Synth. Biol. 2025, 14, 1414−1424

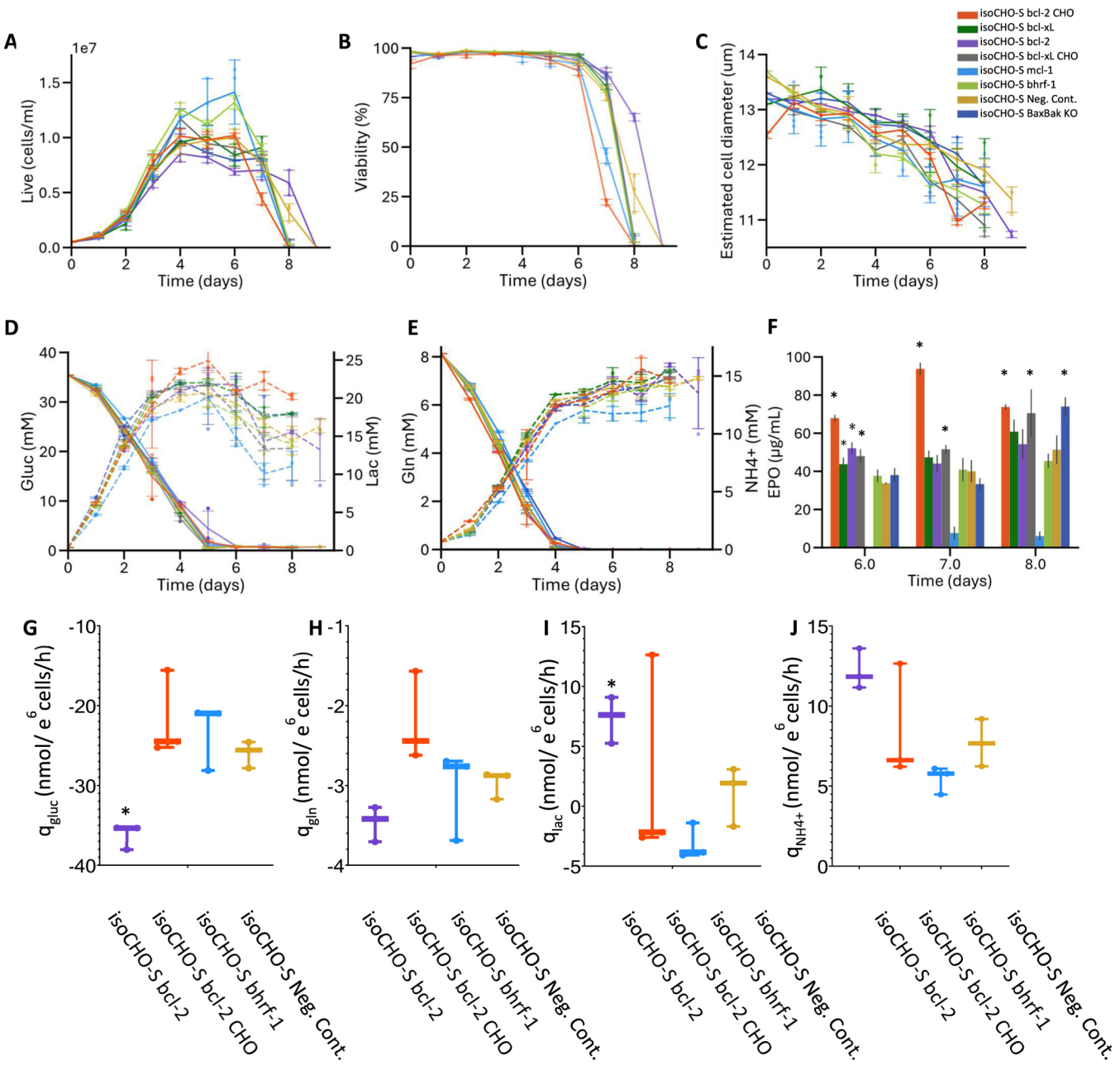

Figure 3. Batch culture of the studied isogenic cell lines. Development overtime of: (A) VCD in cells/mL, (B) viability in %, (C) estimated cell diameter in μm, (D) glucose (solid lines) and lactate (dashed lines) in mM and (E) glutamine (solid lines) and ammonia (dashed lines) in mM. (F) Shows EPO concentration at days 6, 7, and 8. (G–J) presents the glucose, glutamine, lactate, and ammonium consumption/production rate in nmol/ e^6 cells/h for isoCHO-S bcl-2, bcl-2 CHO, bhrf-1, and Neg. Cont. Statistically significant values compared to the negative control with a Dunnett's test are (p-value <0.05) illustrated with "*".

and isoCHO-S bhrf-1 produced the lowest amount of byproducts lactate (Figure 3D) and ammonia (Figure 3E) with statistical significance when compared to isoCHO-S bcl-2 CHO. However, the decline in viability was almost as fast as isoCHO-S bcl-2 CHO (Figure 3B).

In terms of EPO production, both human and CHO bcl-2 and bcl-xL expressing cells achieved a higher titer at day 6, whereas mcl-1 and the two controls showed a lower titer (Figure 3F). On days 7 and 8, the two CHO genes bcl-2 and bcl-xL were significantly higher than controls, while the human equivalents were not. The BaxBak clone caught up by day 8, while the bhrf-1 cell line showed almost no production at any time point. The three isoCHO-S bcl-2 CHO cell lines showed a pronounced peak on day 7, possibly as a result of release from dying cells. This phenomenon was observed in previous studies.[29]

Consumption and production rates for isoCHO-S bcl-2, isoCHO-S bcl-2 CHO, and isoCHO-S bhrf-1 were calculated. Interestingly, isoCHO-S bcl-2 was the only cell line that deviates significantly from the negative control in terms of glucose consumption and lactate production.

While the use of isogenic cell lines facilitated the direct comparison of growth and metabolic effects of antiapoptotic genes, productivity measures are more difficult to interpret given that titers are measured after glutamine and glucose were depleted. It is important to consider the complex interplay between nutrient depletion and cell productivity. Specifically,

https://doi.org/10.1021/acssynbio.4c00382
ACS Synth. Biol. 2025, 14, 1414–1424

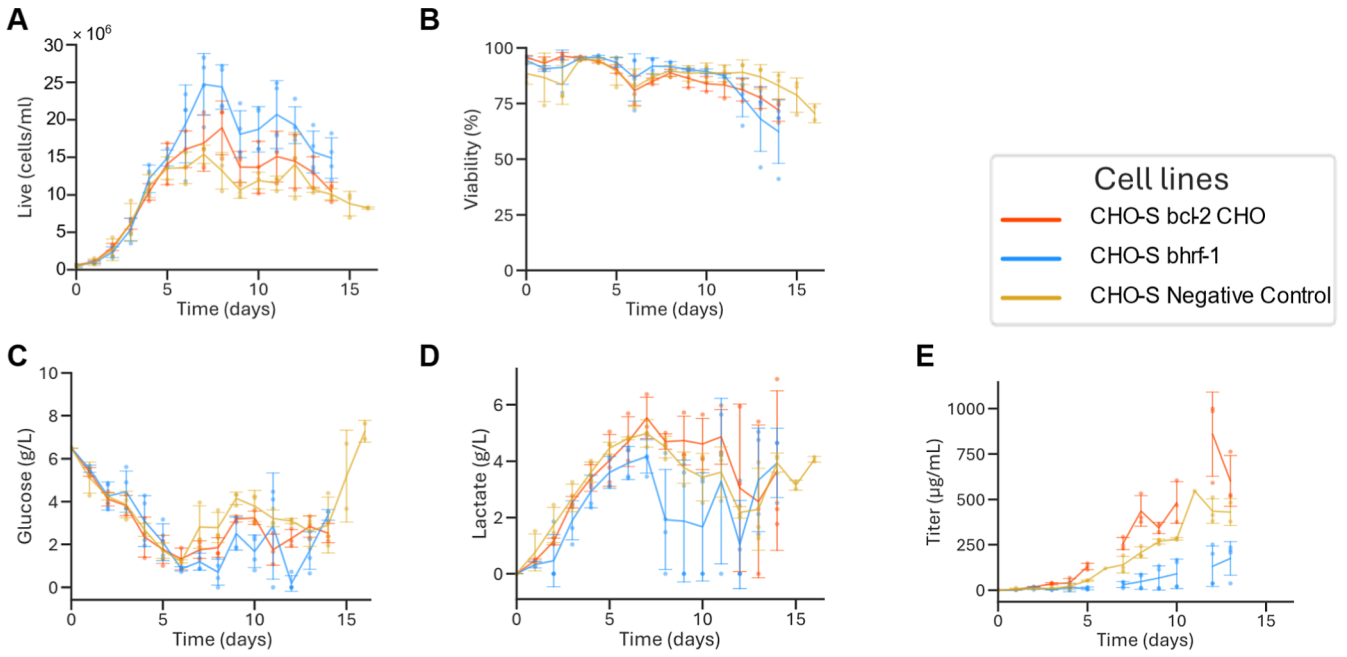

Figure 4. ambr15 fed-batch run for all studied isogenic cell lines. isoCHO-S bcl-2 CHO and isoCHO-S bhrf-1 alongside the isoCHO-S negative control cell line to study possible phenotype changes over the course of the process. (A) VCD in cells/mL, (B) viability in %, (C) glucose in g/L, (D) lactate in g/L, and (E) EPO titer in μg/mL.

the depletion of glutamine can impact cell productivity independently of the antiapoptotic phenotype due to its documented effect on potential EPO degradation.[29] Nevertheless, if this phenomenon occurs, it would likely affect all cell lines equally, thereby maintaining the validity of our comparative results. To further strengthen our findings, future studies could incorporate time-course analyses of productivity before complete nutrient depletion or implement fed-batch cultures to maintain consistent nutrient levels throughout the experiment.

Fed-Batch Cultures Presented Different Phenotypes. Fed-batch cultures are a widely adopted manufacturing strategy wherein nutrients are supplied to compensate for potential nutrient depletion, resulting from cell growth. Consequently, prolonged processes may lead to the overaccumulation of toxic byproducts such as ammonia or lactate. Drawing from the observations in the batch culture, where two interesting profiles emerged among the outliers—bcl-2 CHO exhibiting the highest production and bhrf-1 showcasing the highest VCD alongside unexpected metabolic profiles—we perform a fed-batch in the ambr15 system with three independent subclones for each cell line under pH and temperature-controlled conditions (Figure 4A,D,E).

During the exponential phase of cell growth (from inoculation to day 5), minimal differences were observed in terms of VCD and viability (Figure 4A,B). Hereafter, performances began to diverge, with bhrf-1 achieving the highest VCD while producing the lowest amount of lactate (Figure 4D). This agreed with the previously observed results in the batch mode. Surprisingly, in terms of viability, no significant antiapoptotic behaviors were observed. The negative control outperformed both antiapoptotic cell lines in terms of viability as it reached a similar viability 2 days later than the modified cell lines (Figure 4B). As described in the Introduction, there are many potential factors for the apoptosis, and the reason why the negative control was able to keep its viability for a longer time can be a consequence of other uncontrolled effects. As mentioned before, the lack of nutrients observed in some of the bhrf-1 clones could have triggered unavoidable cell death.

Nevertheless, researchers have established that, although differences between subclones are minimal, they are not entirely absent, and some results may be impacted by these variations.[30] Targeted integration offers the advantage of generating cell lines that are highly similar genotypically, thereby reducing phenotypic variation compared to random integration. As a result, cell lines derived from targeted integration are expected to exhibit fewer differences than those derived from random integration, leading to more consistent and reliable experimental outcomes.

The lack of improvement from bcl-2 CHO was already anticipated by a transcriptional study in 2006, which showed that the expression of bcl-2 does not change during a fed-batch, describing how cell death was potentially being originated from a pathway with no participation of bcl-2.[31] However, it must be noted that the high variability in the lactate profile for bhrf-1 was observed due to some data points falling below the limit of detection.

Interestingly, once again, isoCHO-S bcl-2 CHO outperformed the negative control in terms of the titer measured throughout the culture (Figure 4E). It is important to note that no decrease in EPO titer was observed compared to the batch experiment from the previous section. This phenotype was expected, as low levels of glutamine were reported to lead to EPO degradation over time by proteolysis.[29] Similar glucose consumption (Figure 4C) and lactate production (Figure 4D) to those of the negative control were observed.

Contrary to previously published data, which relied on shake-flask methods to conduct fed-batch experiments, we have, to the best of our knowledge, pioneered the assessment of bcl-2 CHO performance using the ambr15 system. We chose this experimental setup due to its robustness, capability to operate reactors in triplicate, and established track record in scalability.

https://doi.org/10.1021/acssynbio.4c00382
ACS Synth. Biol. 2025, 14, 1414−1424

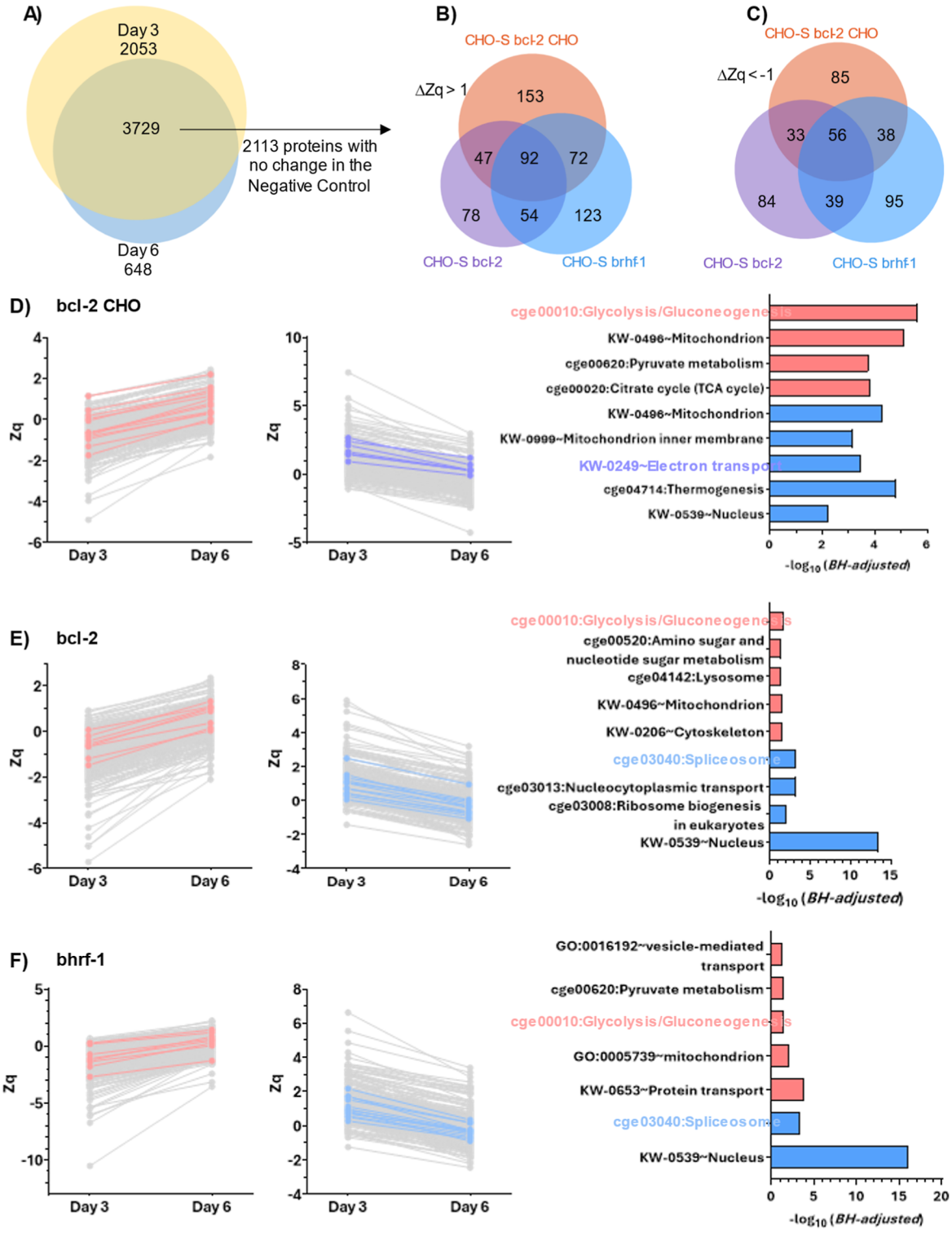

Figure 5. Metabolic differences in isoCHO-S bcl-2, CHO−S bcl-2 CHO, and CHO−S bhrf-1. (A) Venn diagram of proteins identified with more than one peptide in the negative control at day 3 and at day 6. All proteins with a development of less than 1 unit of standardized variable, Z_q, between day 3 and day 6 were excluded for further analysis. (B) Proteins with a $\Delta Z_q > 1$ from days 3−6 and (C) proteins with a $\Delta Z_q \leftarrow 1$ from days 3−6. (D) Shows all proteins from isoCHO-S bcl-2 CHO with (right) $\Delta Z_q \leftarrow 1$ from days 3−6 with proteins belonging to cge00190: oxidative phosphorylation colored in purple, (middle) $\Delta Z_q > 1$ from day 3 to 6 for cge00010:glycolysis/gluconeogenesis colored in red, and (left) relevant pathways selected based on logarithm of adjusted Benjamini score. Red bars indicate enrichment of upregulated processes and blue bars of downregulated process. (E,F) illustrate proteins filtered with the same criteria as figure (D) for bcl-2 and bhrf-1, respectively, with cge03040:spliceosome proteins marked in blue.

Throughout this project, our aim was to establish foundational insights into genetic comparisons, with a particular focus on antiapoptotic cell lines. We believe that transitioning to equipment prioritizing reliability, provided it accommodates the experimental setup, is the optimal approach to achieving our goals.

https://doi.org/10.1021/acssynbio.4c00382
ACS Synth. Biol. 2025, 14, 1414−1424

In conclusion, the beneficial consequences of overexpressing antiapoptotic genes were high VCD and increased titer for isoCHO-S bcl-2 CHO.

Relevant Metabolic Differences Were Observed between Isogenic Cell Lines isoCHO-S bcl-2, bcl-2 CHO, and bhrf-1 Using Proteomics. The different metabolic responses between cell lines warrant a closer investigation of the antiapoptotic responses. For this purpose, we used multiplexed quantitative proteomic analysis to compare bcl-2, bcl-2 CHO, and bhrf-1 using the negative control as a reference. The apoptotic response was observed between the late exponential phase (day 3) and postdepletion of glucose and glutamine but prior to major loss of cell death viability (day 6) in batch culture (Figure 3; specific data points are available in Figure S4).

Only proteins identified with more than one peptide in the negative control on days 3 and 6 were selected for further analysis. We further restricted the analysis to proteins that displayed minimal change from days 3−6 in the negative control ($|\Delta Z_q| < 1$) to focus on proteins that were differentially changing in our studied cell lines and not in the negative control. Among the 3729 identified proteins, 2113 passed the cutoff of $|\Delta Z_q| < 1$ (Figure 5A).

From these 2113 proteins, 619 displayed an increasing trend ($\Delta Z_q > 1$), while 430 demonstrated a decreasing trend ($\Delta Z_q < 1$), in at least one of the modified cell lines. Notably, when visualizing the increasing and decreasing proteins in a Venn diagram, three distinct proteomes emerged (Figure 5B,C), indicating that a significant number of proteins undergoing a specific trend were not shared among all cell lines. For instance, only 92 of 619 showed the same increasing trend in all three cell lines, while 56 of 430 proteins shared a decreasing trend. Consequently, we analyzed each cell line individually using DAVID as an enrichment tool to identify processes that were enhanced in each cell line.[32,33] Specific consumption and production rates were calculated for the range of 3 to 6 days to further discuss some of the obtained enrichment results (Figure S4).

In the case of isoCHO-S bcl-2 CHO, increasing processes include glycolysis/gluconeogenesis (cge0010), mitochondrion (KW-0496), pyruvate metabolism (cge00620), and the citrate cycle (cge00020) (Figure 5D). Out of the 13 overexpressed proteins belonging to the Kegg pathway of glycolysis/gluconeogenesis (cge0010), 3 participate in the citrate cycle and pyruvate metabolism simultaneously [pyruvate dehydrogenase (PDH) E1 component subunit beta (EC 1.2.4.1), acetyltransferase component of PDH complex (EC 2.3.1.12), and phosphoenolpyruvate carboxykinase (PEPCK) (EC 4.1.1.32)] (Table S1). PDH upregulation suggests a lack of available ATP. PEPCK upregulation might be responsible for providing precursors for nucleotide and amino acid biosynthesis.[34] This phenotype might explain some of the features observed in the metabolism of the isoCHO-S bcl-2 CHO. It has been widely reported that when glucose is depleted from the medium, cells begin consuming lactate and, consequently, their metabolism shifts toward pyruvate production.[35−37] This could be implied by the overexpression of these proteins showing a flux coming out of the mitochondria to the cytosol, which can benefit the biosynthesis pathway of different molecules such as amino acids,[34] a pathway that has been positively enriched on isoCHO-S bcl-2 CHO (Figure 5D). Pyruvate can still enter the TCA cycle and be converted to oxalacetate by pyruvate carboxylase as the proteomics analysis was based on relative quantification, and the lack of overexpression indicates that the value is equivalent to the negative control, not that it is absent from the cell. The carbon flux moving toward gluconeogenesis and branching into these diverse biosynthesis pathways might explain the decreased rate of glucose consumption observed in bcl-2 (Figure S4E).

Conversely, the oxidative phosphorylation (KW-0249), thermogenesis (cge04714), mitochondrion inner membrane (KW-0999), and nucleus (KW-0539) significantly decreased over time while they remained constant in the negative control (adjusted BH < 0.05) (Table S2). Considering these results, we hypothesized that the decrease in the oxidative phosphorylation pathway could reduce the availability of H^+ inside the mitochondria, affecting the citrate cycle proton requirements and enhancing the gluconeogenesis instead of the glycolysis. Considering how intertwined all the impacted pathways are and how a decrease of a flux can be compensated with an increase somewhere else, it is important to verify these hypotheses with the aid of more complex studies by, for instance, adding nonradioactive isotope tracers (usually synthetic metabolites labeled with carbon-13 (^{13}C).[38]

Proteins changing in the isoCHO-S bcl-2 cell line (Figure 5E) exhibited development similar to that of isoCHO-S bcl-2 CHO in terms of glycolysis/gluconeogenesis (cge0010) being upregulated. The glucose consumption rate between days 3 and 6 was indeed statistically significantly larger than the negative control, showing a higher consumption of glucose and a higher lactate production (Figure S4E,G). However, pyruvate metabolism (cge00620) and the citrate cycle (cge00020) were not statistically significantly upregulated (adjusted BH > 0.05). Interestingly, cytoskeleton (KW-0206) proteins were upregulated, while nuclear (KW-0539) proteins were downregulated. This might explain why cell size in isoCHO-S bcl-2 CHO is larger on day 6 compared with the negative control (Figure 3C). The decrease in spliceosome (cge03040) and ribosome biogenesis-related (cge03008) proteins is a phenotype related to the lower growth observed in this cell line compared to the other one, as presented in Figure 3A. All results from enrichment analysis are grouped in Tables S3 and S4.

Lastly, proteins changing in the bhrf-1 cell line showed upregulation in glycolysis/gluconeogenesis (cge0010) with 8 proteins and in pyruvate metabolism (cge00620) with 7 proteins (Figure 5F). The decrease of nuclear (KW-0539) proteins mostly translated to the decrease of spliceosome (cge03040) proteins. All upregulated and downregulated processes are available in Tables S5 and S6. The spliceosome is responsible for the removal of introns from nuclear pre-mRNA. However, considering the crucial role of the spliceosome in the proper function of the cell, many proteins are redundant.[39]

Interestingly, although the three modified cell lines all display an upregulation in the glycolysis/gluconeogenesis pathway, only 4 proteins were common in the upregulation: phosphoglucomutase-2, S-(hydroxymethyl) glutathione dehydrogenase, multiple inositol polyphosphate phosphatase 1, and aldo-keto reductase family 1 member A1. These proteins are scattered in the pathway with no direct connection between them, showing that, although the glycolysis/gluconeogenesis was significantly enriched, each cell line acted differently.

The relationship between apoptosis and glycolysis/gluconeogenesis has been reported in the literature for several years, with studies conducted in both engineered CHO cells lines to withstand apoptosis and highly producers cell lines.[40,41] For instance, the study performed by Baik and Lee identified dihydrolipoamide-S-acetyltransferase, while Carlage et al. identified glyceraldehyde-3-phosphate dehydrogenase and alfa-

https://doi.org/10.1021/acssynbio.4c00382
ACS Synth. Biol. 2025, 14, 1414−1424

enolase. Interestingly, although the authors agreed on the relationship between apoptosis and glycolysis, the identified proteins were different. Moreover, these studies were carried out using random integration, making it more difficult to compare and draw conclusions. This highlights the necessity of selecting a common framework in order to compare these studies.

Another interesting detail is that most of the shared overexpressed proteins were localized in the cytoplasm (17 in cytosol, 13 in mitochondrion, and 30 in cytoplasm unspecified), whereas most of the downregulated proteins were localized in the nucleus (15 proteins).

In conclusion, the overexpression of a single gene with apparently the same function but different origin (human, CHO, and viral) resulted in three distinctly different phenotypes. A proteomic analysis facilitated drawing conclusions to explain the different metabolic profiles.

One of the main focuses of molecular biologists has been understanding the effects of overexpression of specific genes and their impact on productivity and metabolism. However, the reliance on random integration has impeded comparisons between different groups and publications. This work demonstrates that while not without its limitations, targeted integration can potentially minimize these challenges. By facilitating more accurate comparisons within the scientific community, targeted integration helps ensure robustness and reproducibility across publications. Additionally, it is important to understand the intrinsic biological variability that any subclones may have and take that into account when analyzing results.

Overall, this study has provided the necessary tools to develop isogenic cell lines for robust gene comparison.

MATERIALS AND METHODS

Cell Culture. CHO−S cell lines (Thermo Fisher Scientific, Waltham, MA, USA) were cultivated in disposable 125 mL polycarbonate shake flasks with a working volume of 30 mL. CD CHO medium (Gibco, Buffalo, NY, United States) was supplemented with 8 mM glutamine (Gibco), 1% of an anticlumping agent (Gibco), and 0.01% of antibiotic−antimycotic 100× (Gibco). Cell cultures were incubated in a 5% CO_2 air mixture at 37 °C in a Heracell 150 incubator (Thermo Fisher) with agitation of 120 rpm by a Celltron shaker (Infors HT, Switzerland) and were passaged every 2 to 3 days to 0.3−0.5 × 10^6 cells/mL to maintain cells in the exponential phase. NucleoCounter-250 (ChemoMetec, Denmark) was employed to determine cell density, viability, and estimated cell diameter following the manufacturer's instructions.

Plasmid Construction. Antiapoptotic genes from human bcl-2, human bcl-xL, mcl-1, and bhrf-1 were codon optimized for *Cricetulus griseus* and supplied by GeneART (Thermo Fisher Scientific). Bcl-2 CHO and bcl-xL CHO were extracted from cDNA from a CHO−S pellet harvested at the midexponential phase. These DNA fragments were then inserted into a backbone plasmid via uracil-specific excision reagent (USER) cloning method.[42]

The designed backbone plasmid had linker sequences for the USER cloning strategy followed by a polyA trap from bovine growth hormone (BGHpA) and was separated from the EPO gene under the relative promoter units (RPU) 100 promoter by 2 chicken b-globin locus control region hypersensitive site 4 (HS4) insulators.

This construct was flanked by loxP (ATAACTTCGTATAGCATACATTATACGAAGTTAT) and lox2272 (ATAACTTCGTATAGGATACTTTATACGAAGTTAT). To facilitate colony selection and amplification in *E. coli* Mach1, the plasmid had the ampicillin resistance gene.

DNA bricks for USER assembly were generated by PCR amplification with Phusion U Hot Start DNA polymerase (Thermo Fisher Scientific) and uracil-containing primers (Integrated DNA Technologies, Coralville, IA, USA). Then, the product of the USER assembly was transformed into *E. coli* Mach1 competent cells (Thermo Fisher Scientific) for plasmid amplification. Sanger sequencing and restriction digestion were used for the verification of all constructs. All plasmid designs are listed in Figure S1.

Cell Line Generation and Verification. We developed all cell lines with relevant antiapoptotic genes following the previously published process for cell line generation by our group.[24] Briefly, the MCL had the mCherry gene flanked by loxP/lox2272 sites to allow for RMCE.[24] The MCL was cotransfected with a plasmid containing EPO flanked by recombination sites loxP and lox2272 and a second plasmid with Cre-recombinase. Successfully recombinant clones switched the mCherry gene for EPO and were single-cell sorted into a flat-bottom Corning 384-well plate (Sigma-Aldrich) containing 30 μL of CD CHO medium with 8 mM glutamine and 1.5% HEPES buffer (Gibco) using the SH800S Cell Sorter (Sony biotechnology, CA, USA) based on the $mCherry^-$ phenotype. A negative control cell line was designed, replacing the mCherry gene for 3 stop codons to ensure that the observed outcomes were not a product of the sorting process.

IsoCHO-S was used when referring to CHO−S cell lines generated via RMCE and when the antiapoptotic gene was coming from CHO, it was added at the end. For instance, isoCHO-S bcl-2 CHO refers to the isogenic CHO−S cell line with one copy of the gene bcl-2 from the CHO origin.

After single-cell sorting, the presence of only one cell per well was assessed with a Celigo Imaging Cell Cytometer (Nexcelom Bioscience). Ten to 14 days after the sorting, subconfluent clones were transferred to flat-bottom 96-well plates with 180 μL of CD CHO medium with 0.01% of antibiotic−antimycotic 100× and 8 mM of glutamine using an epMotion 5070 liquid handling workstation (Eppendorf). Subsequently, cells were expanded to flat-bottom 12-well plates and 125 mL shake flasks for cell banking.

To ensure that gene expression occurs only with successful recombination, promoter EF1α was located before the loxP site. A junction PCR was designed with primers binding at each end of the loxP/lox2272. Clones with a band corresponding to the expected DNA size were selected for qPCR. In this second step, TaqMan Gene Expression Master Mix (Thermo Fisher Scientific), custom-made TaqMan assays for EPO, and one-copy endogenous reference gene C1GALT1C1 (Cosmc)[43] were used in the duplex assay (EPO and Cosmc).

BaxBak KO Generation. All antiapoptotic generated cell lines expressed the bcl-2 family of proteins that prevent the pore-forming activity of Bax and Bak on the mitochondrial membrane. Consequently, we KO the Bax and Bak genes from the negative control cell line, which contained 3 stop codons instead of an antiapoptotic gene, to ensure that any observed differences were solely the consequence of the successful KO. For the generation of the BaxBak KO, the method based on CRISPR/Cas9 editing published by Grav et al. was followed.[44] Briefly, specific single guide RNA (sgRNA) were designed for each gene (GGAAGCCGGTCAAACCACGTTGG for Bak and

https://doi.org/10.1021/acssynbio.4c00382
ACS Synth. Biol. 2025, 14, 1414−1424

GCTGATGGCAACTTCAACTGGGG for Bax) using the CRISPy bioinformatics tool.[45]

The sgRNAs were synthesized, annealed, and cloned to an expression vector backbone harboring scaffold RNA sequence, the U6 promoter and a termination sequence to generate sgRNA expression.[44] The GFP 2A peptide-linked Cas9 (GFP_2A_Cas9) expression plasmid was used.[12] A plasmid containing the sgRNA sequence of interest was cotransfected with the GFP_2A_Cas9 plasmid. Single cell sorting was performed to separate the GFP positive cells. The KO was verified by Sanger sequencing and Western blotting (Figure S3).

NaBu Assay. In order to trigger apoptosis in the genetically engineered cell lines, cells were resuspended in CD CHO supplemented with 8 mM glutamine, 1% of anti-clumping agent, 0.01% of antibiotic−antimycotic, and 20 mM NaBu (Sigma-Aldrich—Merck Life Science B5887−1G LOT/SBLBQ8041 V) to reach a final concentration of 2.5×10^6 cells/mL. Then, cells were seeded in a 6-well plate with a working volume of 3 mL.

Batch Cultivation in 125 mL Shake Flask. Successfully generated cell lines were seeded at 0.5×10^6 cells/mL in 125 mL shake flasks with 30 mL of CD CHO supplemented with 8 mM glutamine, 1% of anti-clumping agent, and 0.01% of antibiotic−antimycotic for the batch characterization.

Daily, 1 mL of cell culture was removed from each shake flask. 50 μL was utilized to measure cell density (cell/mL), viability (%), and estimated cell size (μm) with the NucleoCounter-250. The remaining volume was centrifuged at 1000 g for 1 min, and 400 μL of supernatant was run in the BioProfile FLEX2 (Nova Biomedical, Waltham, MA, USA) for glucose, glutamine, ammonia, and glutamate measurements. The remaining volume from day 3 onward was stored at −80 °C for subsequent EPO titer analysis with an Octet RED96 system (ForteBio, Sartorius, Göttingen, Germany). Finally, the pellet for days 3 and 6 was stored at −80 °C for proteomics study.

Statistical analysis of EPO concentrations obtained from each cell line at days 6, 7, and 8 was performed with GraphPad Prism software (Version 10.02.01, GraphPad Software, San Diego, CA) using a Dunnett's test with the negative control cell line as the control.

Fed-Batch in the ambr15 System. Three cell lines were further characterized in a fed-batch culture that was run in the ambr15 system (Sartorius, Göttingen, Germany). Three bioreactors were inoculated for each cell line (isoCHO-S bcl-2 CHO, CHO−S bhrf-1, and isoCHO-S negative control) at 0.5×10^6 cells/mL with 13 mL of 8 mM glutamine, 1% of anti-clumping agent, and 0.01% of antibiotic−antimycotic. Daily, 0.2 μL of anticlumping agent was added to each vessel to prevent foam accumulation.

Proteomics Study. Protein identification was performed as described previously.[46] Briefly, MS/MS scans were matched against *C. griseus* (UniProtKB/Swiss-Prot 2023_10 Release). Sequences of eGFP and Bhrf-1 were added to the previous database to enable their identification. For comparative analysis of changes in protein abundance, we applied weighted scan−peptide−protein statistical workflow, using the SanXoT package.[47−49]

The quantitative information is, as detailed by Lavado-García et al. 2020, obtained from the spectra and used to quantify the peptides from which the spectra are produced and then the proteins that generate these peptides.[50] These standardized variables (Z_q) express the quantitative values in units of standard deviation.[49] The quantified proteins were functionally annotated by using the gene ontology (GO) database. For further GO annotation, the database for annotation, visualization, and integrated discovery (DAVID) was used to perform functional enrichment analysis and to extract adjusted Benjamini scores for the enriched processes.[51]

Specific consumption and production rates were calculated, as indicated in eq 1, where x_f equals the final concentration of the metabolite of interest, x_0 equals the initial concentration of the metabolite of interest, t_f final time, t_0 initial time, VCD_0 VCD at initial time, and VCD_f VCD at final time

$$q_x = \frac{x_f - x_0}{\frac{(t_f - t_0) \times (VCD_0 + VCD_f)}{2}} \quad (1)$$

Considering that the sampling points for the proteomics analysis were days 3 and 6, initial time equals 3, and final time equals 6 in the previous formula.

Statistical Analysis. Relevant values for specific productivity and consumption were compared with a one-way analysis of variance via GraphPad Prism software (Version 10.02.01, GraphPad Software, San Diego, CA). When the results of the analysis showed that the means were statistically significant, a Dunnett's test was used to compare relevant means against the negative control. A star (*) was added when the change was statistically significant with a p-value <0.05.

■ ASSOCIATED CONTENT

Supporting Information

The Supporting Information is available free of charge at https://pubs.acs.org/doi/10.1021/acssynbio.4c00382.

Plasmid map of the backbones used in the development of the cell lines; junction PCR results to verify successful clone generation followed by the western blotting used in the confirmation of the Bax/Bak KOs; development of live cells, viability, estimated cell diameter, glucose, lactate, glutamine, and ammonia from days 3−6; specific consumption and production rated calculated for each metabolite and cell line; and western blots to ensure protein expression of the introduced genes of interest (PDF)

Results from DAVID enrichment of upregulated and downregulated proteins for CHO-S bcl-2 CHO, CHO-S bcl-2, CHO-S bhrf-1, and CHO-S bhrf-1 (XLSX)

■ AUTHOR INFORMATION

Corresponding Author

Jesús Lavado-García − *The Novo Nordisk Foundation Center for Biosustainability, Technical University of Denmark, Lyngby 2800, Denmark;* orcid.org/0000-0001-9993-6332; Email: jlavgar@dtu.dk

Authors

David Catalán-Tatjer − *The Novo Nordisk Foundation Center for Biosustainability, Technical University of Denmark, Lyngby 2800, Denmark;* orcid.org/0000-0002-0900-9912

Saravana Kumar Ganesan − *The Novo Nordisk Foundation Center for Biosustainability, Technical University of Denmark, Lyngby 2800, Denmark*

Iván Martínez-Monje − *The Novo Nordisk Foundation Center for Biosustainability, Technical University of Denmark, Lyngby 2800, Denmark*

Lise M. Grav − *The Novo Nordisk Foundation Center for Biosustainability, Technical University of Denmark, Lyngby 2800, Denmark;* orcid.org/0000-0001-8042-7108

Lars K. Nielsen − *The Novo Nordisk Foundation Center for Biosustainability, Technical University of Denmark, Lyngby 2800, Denmark; Australian Institute for Bioengineering and Nanotechnology, The University of Queensland, Brisbane 4072, Australia;* orcid.org/0000-0001-8191-3511

Complete contact information is available at: https://pubs.acs.org/10.1021/acssynbio.4c00382

Author Contributions

D.C.T.: experimentation, investigation, visualization, writing original draft, and review and editing. S.G.: experimentation. I.M.M. and L.G.: experimental design and conceptualization. J.L.G.: conceptualization, visualization, supervision, and review and editing. L.K.N.: supervision and review.

Notes

The authors declare no competing financial interest.

■ ACKNOWLEDGMENTS

The authors would like to acknowledge generous support by the Novo Nordisk Foundation. This work was supported by NNF20CC0035580 and NNF20SA0066621. L.K.N. is supported by NNF14OC0009473. JLG is supported by NNF22OC0078741 and Marie Skłodowska-Curie Actions (MSCA) Postdoctoral Fellowship 101105465.

■ REFERENCES

(1) Al-Rubeai, M.; Rabinder, P. S.; Singh, R. P.; Singh, R. P.; Mohamed, A.-R.; Rabinder, P. S. Apoptosis in Cell Culture. *Curr. Opin. Biotechnol.* **1998**, *9* (2), 152−156.

(2) Singh, R.; Letai, A.; Sarosiek, K. Regulation of Apoptosis in Health and Disease: The Balancing Act of BCL-2 Family Proteins. *Nat. Rev. Mol. Cell Biol.* **2019**, *20* (3), 175−193.

(3) Krampe, B.; Al-Rubeai, M. Cell Death in Mammalian Cell Culture: Molecular Mechanisms and Cell Line Engineering Strategies. *Cytotechnology* **2010**, *62* (3), 175−188.

(4) Singh, R. P.; Al-Rubeai, M.; Gregory, C. D.; Emery, A. N. Cell Death in Bioreactors: A Role for Apoptosis. *Biotechnol. Bioeng.* **1994**, *44* (6), 720−726.

(5) Rahimi, A.; Karimipoor, M.; Mahdian, R.; Alipour, A.; Hosseini, S.; Kaghazian, H.; Abbasi, A.; Shahsavarani, H.; Shokrgozar, M. A.; Shokrgozar, M. A. Targeting Caspase-3 Gene in rCHO Cell Line by CRISPR/Cas9 Editing Tool and Its Effect on Protein Production in Manipulated Cell Line. *Iran. J. Biotechnol.* **2023**, *21* (1), 75−86.

(6) Ochoa, S. A New Approach for Finding Smooth Optimal Feeding Profiles in Fed-Batch Fermentations. *Biochem. Eng. J.* **2016**, *105*, 177−188.

(7) Bibila, T. A.; Robinson, D. K. In Pursuit of the Optimal Fed-Batch Process for Monoclonal Antibody Production. *Biotechnol. Prog.* **1995**, *11* (1), 1−13.

(8) Bielser, J. M.; Wolf, M.; Souquet, J.; Broly, H.; Morbidelli, M. Perfusion Mammalian Cell Culture for Recombinant Protein Manufacturing − A Critical Review. *Biotechnol. Adv.* **2018**, *36* (4), 1328−1340.

(9) Clincke, M. F.; Mölleryd, C.; Zhang, Y.; Lindskog, E.; Walsh, K.; Chotteau, V. Very High Density of CHO Cells in Perfusion by ATF or TFF in WAVE Bioreactor™: Part I: Effect of the Cell Density on the Process. *Biotechnol. Prog.* **2013**, *29* (3), 754−767.

(10) O'Flaherty, R.; Bergin, A.; Flampouri, E.; Mota, L. M.; Obaidi, I.; Quigley, A.; Xie, Y.; Butler, M. Mammalian Cell Culture for Production of Recombinant Proteins: A Review of the Critical Steps in Their Biomanufacturing. *Biotechnol. Adv.* **2020**, *43* (April), 107552.

(11) Altamirano, C.; Paredes, C.; Cairó, J. J.; Gòdia, F. Improvement of CHO Cell Culture Medium Formulation: Simultaneous Substitution of Glucose and Glutamine. *Biotechnol. Prog.* **2000**, *16* (1), 69−75.

(12) Grav, L. M.; Lee, J. S.; Gerling, S.; Kallehauge, T. B.; Hansen, A. H.; Kol, S.; Lee, G. M.; Pedersen, L. E.; Kildegaard, H. F. One-Step Generation of Triple Knockout CHO Cell Lines Using CRISPR/Cas9 and Fluorescent Enrichment. *Biotechnol. J.* **2015**, *10* (9), 1446−1456.

(13) MacDonald, M. A.; Barry, C.; Groves, T.; Martínez, V. S.; Gray, P. P.; Baker, K.; Shave, E.; Mahler, S.; Munro, T.; Marcellin, E.; Nielsen, L. K. Modeling Apoptosis Resistance in CHO Cells with CRISPR-Mediated Knockouts of Bak1, Bax, and Bok. *Biotechnol. Bioeng.* **2022**, *119* (6), 1380−1391.

(14) Henry, M. N.; MacDonald, M. A.; Orellana, C. A.; Gray, P. P.; Gillard, M.; Baker, K.; Nielsen, L. K.; Marcellin, E.; Mahler, S.; Martínez, V. S. Attenuating Apoptosis in Chinese Hamster Ovary Cells for Improved Biopharmaceutical Production. *Biotechnol. Bioeng.* **2020**, *117* (4), 1187−1203.

(15) Majors, B. S.; Betenbaugh, M. J.; Pederson, N. E.; Chiang, G. G. Mcl-1 Overexpression Leads to Higher Viabilities and Increased Production of Humanized Monoclonal Antibody in Chinese Hamster Ovary Cells. *Biotechnol. Prog.* **2009**, *25* (4), 1161−1168.

(16) Fussenegger, M.; Fassnacht, D.; Schwartz, R.; Zanghi, J. A.; Graf, M.; Bailey, J. E.; Pörtner, R. Regulated Overexpression of the Survival Factor Bcl-2 in CHO Cells Increases Viable Cell Density in Batch Culture and Decreases DNA Release in Extended Fixed-Bed Cultivation. *Cytotechnology* **2000**, *32* (1), 45−61.

(17) Xiong, K.; Marquart, K. F.; la Cour Karottki, K. J.; Li, S.; Shamie, I.; Lee, J. S.; Gerling, S.; Yeo, N. C.; Chavez, A.; Lee, G. M.; Lewis, N. E.; Kildegaard, H. F. Reduced Apoptosis in Chinese Hamster Ovary Cells via Optimized CRISPR Interference. *Biotechnol. Bioeng.* **2019**, *116* (7), 1813−1819.

(18) Templeton, N.; Lewis, A.; Dorai, H.; Qian, E. A.; Campbell, M. P.; Smith, K. D.; Lang, S. E.; Betenbaugh, M. J.; Young, J. D. The Impact of Anti-Apoptotic Gene Bcl-2Δ Expression on CHO Central Metabolism. *Metab. Eng.* **2014**, *25*, 92−102.

(19) Juanola, S.; Vives, J.; Milián, E.; Prats, E.; Cairó, J. J.; Gòdia, F. Expression of BHRF1 Improves Survival of Murine Hybridoma Cultures in Batch and Continuous Modes. *Appl. Microbiol. Biotechnol.* **2009**, *83* (1), 43−57.

(20) Majors, B. S.; Betenbaugh, M. J.; Pederson, N. E.; Chiang, G. G. Enhancement of Transient Gene Expression and Culture Viability Using Chinese Hamster Ovary Cells Overexpressing Bcl-xL. *Biotechnol. Bioeng.* **2008**, *101* (3), 567−578.

(21) Han, Y. K.; Ha, T. K.; Kim, Y.-G.; Lee, G. M. Bcl-XL Overexpression Delays the Onset of Autophagy and Apoptosis in Hyperosmotic Recombinant Chinese Hamster Ovary Cell Cultures. *J. Biotechnol.* **2011**, *156* (1), 52−55.

(22) Mastrangelo, A. J.; Hardwick, J. M.; Bex, F.; Betenbaugh, M. J. Part I. Bcl-2 and Bcl-X(L) Limit Apoptosis upon Infection with Alphavirus Vectors. *Biotechnol. Bioeng.* **2000**, *67* (5), 544−554.

(23) Ko, P.; Misaghi, S.; Hu, Z.; Zhan, D.; Tsukuda, J.; Yim, M.; Sanford, M.; Shaw, D.; Shiratori, M.; Snedecor, B.; Laird, M.; Shen, A. Probing the Importance of Clonality: Single Cell Subcloning of Clonally Derived CHO Cell Lines Yields Widely Diverse Clones Differing in Growth, Productivity, and Product Quality. *Biotechnol. Prog.* **2018**, *34* (3), 624−634.

(24) Grav, L. M.; Sergeeva, D.; Lee, J. S.; de Mas, I. M.; Lewis, N. E.; Andersen, M. R.; Nielsen, L. K.; Lee, G. M.; Kildegaard, H. F. Minimizing Clonal Variation during Mammalian Cell Line Engineering for Improved Systems Biology Data Generation. *ACS Synth. Biol.* **2018**, *7* (9), 2148−2159.

(25) Lee, J. S.; Kallehauge, T. B.; Pedersen, L. E.; Kildegaard, H. F. Site-Specific Integration in CHO Cells Mediated by CRISPR/Cas9 and Homology-Directed DNA Repair Pathway. *Sci. Rep.* **2015**, *5*, 8572.

(26) Yee, J. C.; de Leon Gatti, M.; Philp, R. J.; Yap, M.; Hu, W. S. Genomic and Proteomic Exploration of CHO and Hybridoma Cells under Sodium Butyrate Treatment. *Biotechnol. Bioeng.* **2008**, *99* (5), 1186−1204.

(27) Wang, M. D.; Yang, M.; Huzel, N.; Butler, M. Erythropoietin Production from CHO Cells Grown by Continuous Culture in a Fluidized-Bed Bioreactor. *Biotechnol. Bioeng.* **2002**, *77* (2), 194−203.
(28) Avello, V.; Torres, M.; Vergara, M.; Berrios, J.; Valdez-Cruz, N. A.; Acevedo, C.; Sampayo, M. M.; Dickson, A. J.; Altamirano, C. Enhanced Recombinant Protein Production in CHO Cell Continuous Cultures under Growth-Inhibiting Conditions Is Associated with an Arrested Cell Cycle in G1/G0 Phase. *PLoS One* **2022**, *17* (11), 02776200.
(29) Yang, M.; Butler, M. Enhanced Erythropoietin Heterogeneity in a CHO Culture Is Caused by Proteolytic Degradation and Can Be Eliminated by a High Glutamine Level. *Cytotechnology* **2000**, *34* (1−2), 83−99.
(30) Weinguny, M.; Klanert, G.; Eisenhut, P.; Lee, I.; Timp, W.; Borth, N. Subcloning Induces Changes in the DNA-Methylation Pattern of Outgrowing Chinese Hamster Ovary Cell Colonies. *Biotechnol. J.* **2021**, *16* (6), 1−13.
(31) Wong, D. C. F.; Wong, K. T. K.; Lee, Y. Y.; Morin, P. N.; Heng, C. K.; Yap, M. G. S. Transcriptional Profiling of Apoptotic Pathways in Batch and Fed-batch CHO Cell Cultures. *Biotechnol. Bioeng.* **2006**, *94* (2), 373−382.
(32) Sherman, B. T.; Hao, M.; Qiu, J.; Jiao, X.; Baseler, M. W.; Lane, H. C.; Imamichi, T.; Chang, W. DAVID: A Web Server for Functional Enrichment Analysis and Functional Annotation of Gene Lists (2021 Update). *Nucleic Acids Res.* **2022**, *50* (W1), W216−W221.
(33) Huang, D. W.; Sherman, B. T.; Lempicki, R. A. Systematic and Integrative Analysis of Large Gene Lists Using DAVID Bioinformatics Resources. *Nat. Protoc.* **2009**, *4* (1), 44−57.
(34) Yu, S.; Meng, S.; Xiang, M.; Ma, H. Phosphoenolpyruvate Carboxykinase in Cell Metabolism: Roles and Mechanisms beyond Gluconeogenesis. *Mol. Metab.* **2021**, *53* (May), 101257.
(35) Kumar, S.; Dhara, V. G.; Orzolek, L. D.; Hao, H.; More, A. J.; Lau, E. C.; Betenbaugh, M. J. Elucidating the Impact of Cottonseed Hydrolysates on CHO Cell Culture Performance through Transcriptomic Analysis. *Appl. Microbiol. Biotechnol.* **2021**, *105* (1), 271−285.
(36) Martínez-Monge, I.; Comas, P.; Triquell, J.; Casablancas, A.; Lecina, M.; Paredes, C. J.; Cairó, J. J. Concomitant Consumption of Glucose and Lactate: A Novel Batch Production Process for CHO Cells. *Biochem. Eng. J.* **2019**, *151* (April), 107358.
(37) Martínez, V. S.; Dietmair, S.; Quek, L.; Hodson, M. P.; Gray, P.; Nielsen, L. K. Flux Balance Analysis of CHO Cells before and after a Metabolic Switch from Lactate Production to Consumption. *Biotechnol. Bioeng.* **2013**, *110* (2), 660−666.
(38) Coulet, M.; Kepp, O.; Kroemer, G.; Basmaciogullari, S. Metabolic Profiling of CHO Cells during the Production of Biotherapeutics. *Cells* **2022**, *11* (12), 1929−2021.
(39) Wahl, M. C.; Will, C. L.; Lührmann, R. The Spliceosome: Design Principles of a Dynamic RNP Machine. *Cell* **2009**, *136* (4), 701−718.
(40) Baik, J. Y.; Lee, G. M. A DIGE Approach for the Assessment of Differential Expression of the CHO Proteome under Sodium Butyrate Addition: Effect of Bcl-XL Overexpression. *Biotechnol. Bioeng.* **2010**, *105* (2), 358−367.
(41) Carlage, T.; Hincapie, M.; Zang, L.; Lyubarskaya, Y.; Madden, H.; Mhatre, R.; Hancock, W. S. Proteomic Profiling of a High-Producing Chinese Hamster Ovary Cell Culture. *Anal. Chem.* **2009**, *81* (17), 7357−7362.
(42) Lund, A. M.; Kildegaard, H. F.; Petersen, M. B. K.; Rank, J.; Hansen, B. G.; Andersen, M. R.; Mortensen, U. H. A Versatile System for USER Cloning-Based Assembly of Expression Vectors for Mammalian Cell Engineering. *PLoS One* **2014**, *9* (5), No. e96693.
(43) Yang, Z.; Halim, A.; Narimatsu, Y.; Jitendra Joshi, H.; Steentoft, C.; Gram Schjoldager, K. T.-B.; Alder Schulz, M.; Sealover, N. R.; Kayser, K. J.; Paul Bennett, E.; Levery, S. B.; Vakhrushev, S. Y.; Clausen, H. The GalNAc-Type O-Glycoproteome of CHO Cells Characterized by the SimpleCell Strategy. *Mol. Cell. Proteomics* **2014**, *13* (12), 3224−3235.
(44) Grav, L. M.; la Cour Karottki, K. J.; Lee, J. S.; Kildegaard, H. F. Application of CRISPR/Cas9 Genome Editing to Improve Recombinant Protein Production in CHO Cells. *Methods Mol. Biol.* **2017**, *1603*, 101−118.
(45) Ronda, C.; Pedersen, L. E.; Hansen, H. G.; Kallehauge, T. B.; Betenbaugh, M. J.; Nielsen, A. T.; Kildegaard, H. F. Accelerating Genome Editing in CHO Cells Using CRISPR Cas9 and CRISPy, a Web-Based Target Finding Tool. *Biotechnol. Bioeng.* **2014**, *111* (8), 1604−1616.
(46) Lavado-García, J.; Jorge, I.; Cervera, L.; Vázquez, J.; Gòdia, F. Multiplexed Quantitative Proteomic Analysis of HEK293 Provides Insights into Molecular Changes Associated with the Cell Density Effect, Transient Transfection, and Virus-Like Particle Production. *J. Proteome Res.* **2020**, *19* (3), 1085−1099.
(47) Trevisan-Herraz, M.; Bagwan, N.; García-Marqués, F.; Rodriguez, J. M.; Jorge, I.; Ezkurdia, I.; Bonzon-Kulichenko, E.; Vázquez, J. SanXoT: A Modular and Versatile Package for the Quantitative Analysis of High-Throughput Proteomics Experiments. *Bioinformatics* **2019**, *35* (9), 1594−1596.
(48) Martínez-Acedo, P.; Núñez, E.; Gómez, F. J. S.; Moreno, M.; Ramos, E.; Izquierdo-Álvarez, A.; Miró-Casas, E.; Mesa, R.; Rodriguez, P.; Martínez-Ruiz, A.; Dorado, D. G.; Lamas, S.; Vázquez, J. A Novel Strategy for Global Analysis of the Dynamic Thiol Redox Proteome. *Mol. Cell. Proteomics* **2012**, *11* (9), 800−813.
(49) Navarro, P.; Trevisan-Herraz, M.; Bonzon-Kulichenko, E.; Núñez, E.; Martínez-Acedo, P.; Pérez-Hernández, D.; Jorge, I.; Mesa, R.; Calvo, E.; Carrascal, M.; Hernáez, M. L.; García, F.; Bárcena, J. A.; Ashman, K.; Abian, J.; Gil, C.; Redondo, J. M.; Vázquez, J. General Statistical Framework for Quantitative Proteomics by Stable Isotope Labeling. *J. Proteome Res.* **2014**, *13* (3), 1234−1247.
(50) García-Marqués, F.; Trevisan-Herraz, M.; Martínez-Martínez, S.; Camafeita, E.; Jorge, I.; Lopez, J. A.; Méndez-Barbero, N.; Méndez-Ferrer, S.; Del Pozo, M. A.; Ibáñez, B.; Andrés, V.; Sánchez-Madrid, F.; Redondo, J. M.; Bonzon-Kulichenko, E.; Vázquez, J. A Novel Systems-Biology Algorithm for the Analysis of Coordinated Protein Responses Using Quantitative Proteomics. *Mol. Cell. Proteomics* **2016**, *15* (5), 1740−1760.
(51) Benjamini, Y.; Hochberg, Y. Controlling the False Discovery Rate: A Practical and Powerful Approach to Multiple Testing Author (s): Yoav Benjamini and Yosef Hochberg Source: Journal of the Royal Statistical Society. Series B (Methodological). *J. Roy. Stat. Soc. B* **1995**, *57* (1), 289−300.

https://doi.org/10.1021/acssynbio.4c00382
ACS Synth. Biol. 2025, 14, 1414−1424